Bulletin of Mathematical Biology, Vol. 59, No. 2, pp. 263–294, 1997
Elsevier Science Inc.

0092-8240/97 $17.00 + 0.00

S0092-8240(96)00072-9

ON THE ORIGIN OF TIGER BUSH

■ R. LEFEVER and O. LEJEUNE
Service de Chimie-Physique, CP 231,
Université Libre de Bruxelles,
B-1050 Bruxelles, Belgium

(*E.mail: rlevever@ulb.ac.be, olejeune@ulb.ac.be*)

We propose a model which describes the dynamics of vast classes of terrestrial plant communities growing in arid or semi-arid regions throughout the world. On the basis of this model, we show that the vegetation stripes (*tiger bush*) formed by these communities result from an interplay between short-range cooperative interactions controlling plant reproduction and long-range self-inhibitory interactions originating from plant competition for environmental resources. Isotropic as well as anisotropic environmental conditions are discussed. We find that vegetation stripes tend to orient themselves in the direction parallel or perpendicular with respect to a direction of anisotropy depending on whether this anisotropy influences the interactions favouring or inhibiting plant reproduction; furthermore, we show that ground curvature is not a necessary condition for the appearance of arcuate vegetation patterns. In agreement with *in situ* observations, we find that the width of vegetated bands increases when environmental conditions get more arid and that patterns formed of stripes oriented parallel to the direction of a slope are static, while patterns which are perpendicular to this direction exhibit an upslope motion. © *1997 Society for Mathematical Biology*

1. Introduction. For a long time, it has been known in the field of plant ecology that many plant communities exhibit non-uniform, non-random vegetation distributions, usually called *vegetation patterns* (Greig-Smith, 1979). Tiger bush (TB) belongs to this class of botanical organisations. It was described for the first time 46 years ago by Macfadyen (1950a, b) in British Somaliland, but since then, it has been observed in many regions throughout the world (White, 1971). By its spatial regularity, by the vastness of the territories which it covers, by the variety of its constitutive plants, as well as by the variety of soils on which it is found, TB is a remarkable and puzzling phenomenon. Its properties summarise as follows:

1. Often undetectable on the ground, it is clearly visible on air photographs such as Fig. 1. It corresponds to amazingly regular patterns in which more or less densely populated vegetation stripes (also often called *vegetation bands*) alternate with stripes of sparsely covered or even bare ground. These patterns may extend over several square kilometers. Their aspect, which usually reminds of the coat markings of the tiger, is at the origin of their name (Clos-Arceduc, 1956).

Figure 1. Stripes of *Acacia bussei* bush in Go-Gub area of Somaliland (reproduced from Boaler and Hodge, 1962). The bands of dense vegetation (dark) are approximately 100 m wide. The width of the separating lanes (bright) is about 50 m.

2. Its existence has been reported in many regions of the Australian, African and American continents. In fact, it is a landscape which may appear in most of the arid and semi-arid regions covering approximately one-third of the emerged surfaces of the earth (White, 1971; Schlesinger *et al.*, 1990). The climate of these regions is characterised by few but intense rains of short duration (Boaler and Hodge, 1964). The annual rainfall ranges from 50 to 750 mm (White, 1969, 1970).
3. The composition of its vegetation may vary considerably from one geographical region to another. The stripes may entirely consist of grass (Worrall, 1959), of grass and scrub (Van Der Meulen and Morris, 1979), or predominantly of trees and bushes (Macfadyen, 1950b; Worrall, 1960b). In fact, the phenomenon is not specific to a particular kind of vegetation (Bernd, 1978). It is also not specific to a particular kind of soil. It has been described on soils ranging from sandy (Worrall, 1960a; Clayton, 1966; Wickens and Collier, 1971) and silty (White, 1969) to clayey (Worrall, 1959; Hemming, 1965).

4. Often, the ground surface slopes gently from 1 m in 500 m up to 1 m in 50 m (Mabbutt and Fanning, 1987). This favours water flowing without drainage channel formation (Greenwood, 1957; Boaler and Hodge, 1964; Montaña, 1992). According to its orientation with respect to (w.r.t.) this slope, TB divides in two classes (Macfadyen, 1950b; Greenwood, 1957; Boaler and Hodge, 1962; White, 1969): (a) the one which is oriented orthogonally to the ground slope, i.e., parallel to the contour lines; (b) the one which runs down parallel to the ground slope. Furthermore, an upslope migration of class (a) stripes has been observed for grass patterns (Worrall, 1959). Similar upslope motion seems also to occur with patterns constituted of trees and bushes, but on a much slower time scale (Greenwood, 1957; Cornet *et al.*, 1988; Tongway and Ludwig, 1990; Montaña, 1992). When the ground surface is practically flat, the vegetation bands are oriented w.r.t. neighbouring declivities or, in their absence, w.r.t. the system borders (Clos-Arceduc, 1964; White, 1970).
5. Comparing patterns in regions of increasing aridity shows that the stripes wavelength increases while simultaneously the average vegetation density decreases (Gavaud, 1966; White, 1970). An inverse correlation between the stripes wavelength and the ground slope has also been put into evidence (Valentin *et al.*, 1996; Eddy *et al.*, 1996).

Some environmental factors which come immediately to mind in looking for causes capable of explaining the formation of TB can easily be discarded: namely, that TB originates from non-uniformities in the spatial distribution of precipitation, from man activities (Worrall, 1960a; Wickens and Collier, 1971), or from soil heterogeneities (Grove, 1957; Beard, 1967). Given that the periodicities involved are typically in the 10-to-100-m range, it is reasonable to consider that, on that scale, the distribution of rainfall is uniform, which excludes the first possible cause mentioned above. On the other hand, nearly all sites where vegetation patterns have been described are (or were until recent times) totally uninhabited by man, which excludes the second possible cause. As far as soil heterogeneities are concerned, the underlying bedrock is, in general, homogeneous at the scale of the pattern wavelength; the soil differences existing between the vegetation bands and the sparser lanes mainly consist in organic content differences due to the vegetation itself (White, 1971). Moreover, it is unrealistic to imagine that an intrinsic feature of the soil is moving upslope and accounts for the upward shifting which has been recorded in the case of some patterns. The third putative cause is therefore excluded as well.

In the following, given that the existence of TB is not due to this sort of external factors, that it is not restricted to a particular kind of soil or a particular kind of vegetation, given also the overall common spatio-temporal characteristics exhibited by TB in many different geographical

regions, we will suppose that the mechanism underlying the formation of these structures is unique, of an intrinsically dynamical nature, and originates from inter-plant interactions operating at the population level. Though introduced by some of the earliest works devoted to TB (see, e.g., Clos-Arceduc, 1964; White, 1971; Greig-Smith, 1979), this idea remains a hypothesis and a subject of debate in the literature, the main reason being that its confirmation (or refutation) meets with considerable practical difficulties on the experimental side. The latter are inherent to the complexity of plant communities and to the very long time scales, by human standards, which govern the evolution of these systems. As a consequence, devising *in situ* experiments capable of determining which effects, if any, a multitude of systemic and environmental factors have on the vegetation distribution is a highly problematic task; it is an even more problematic one to quantify these effects (think, e.g., of quantifying the effects of such factors as the variability of soils, the presence or absence of slopes on the territory, the direction and intensity of dominant winds, the light availability, the presence of termites or of other agents having an influence on soil irrigation and humidity, the occurrence of fires, etc...).

Theory, on the other hand, has up to now played a limited role in the debate concerning the genesis of TB. Unformalised theories, describing the phenomenon in qualitative terms, have been developed and progressively formalised (Greig-Smith, 1979; Ambouta, 1984; Wilson and Agnew, 1992; Mauchamp *et al.*, 1994; Thiéry *et al.*, 1995). So far, however, there exists no theoretical study which investigates the idea that TB has a strictly intrinsic origin, which supports this idea by suggesting a mechanism capable of generating vegetation bands without assuming some environmental spatial anisotropy (especially, a ground slope) and, above all, which provides explicit expressions for the wavelength of these bands in terms of a small number of kinetic parameters. The population dynamics model presented in this paper fills this theoretical gap. It allows us to predict that uniform distributions of vegetation may undergo a symmetry breaking instability as a result of the competition between short-range and long-range inter-plant interactions. The parameters pertinent for describing this instability correspond to properties of the vegetation rather than of the environment: they refer principally to the ranges of inter-plant interactions, to the plant reproduction rate and average lifetime; they are independent from such environmental constraints as boundary conditions or territorial geometries. It is our hope that the identification of these parameters, and the predictions made below concerning the changes in properties which accompany their variations, will feedback on the experimental side and stimulate the development of *in situ* investigations concerning the population dynamics aspects of vegetation patterns.

Modeling the dynamics of vegetal populations is, however, a problem in itself, even if one forgets about the questions raised by vegetation patterns.

The unusual point to be dealt with from a theoretical point of view is that, since individual plants lack mobility, the spatial propagation of plant communities over a territory depends in the first place upon their mechanism of reproduction (e.g., via seeds)[1]. This *propagation-by-reproduction* relationship constitutes a *transport process* without equivalent outside of the vegetal kingdom. Its description needs an innovative modeling effort. Recent attempts in that direction are due to Mauchamp *et al.* (1994) and Thiéry *et al.* (1995). Using a discrete cellular automata kind of model, these authors have been able to simulate numerically the spatial propagation of vegetation. The formation of banded vegetation patterns has also been investigated within this framework of approach (Thiéry *et al.*, 1995). In the present paper, we endeavour to tackle the problem along another, more analytical, line of approach inspired by the mean-field theory of phase transitions in physical systems (see the extension of Turing ideas via an interaction-redistribution formulation discussed by Levin and Segel (1985) for the application of a similar treatment in another context). Concerning this line of approach, let us remark in passing that the use of physical and mathematical methods to investigate the formation of vegetation patterns is encouraged by Macfadyen himself, the discoverer of TB. In one of his papers, he notes indeed (Macfadyen, 1950b): *They* (TB) *are manifestly within the province of botany and ecology*; *the essential background concerns geomorphology and meteorology*; *the causes as I believe, must be investigated by physics and mathematics*. We can only wish that somehow the theory reported below contributes to demonstrate the insightfulness of this statement.

In the next section, we formulate an evolution equation for the vegetation density of plant communities. The salient feature of this equation is that it takes into account the non-local character of the cooperative and self-inhibitory interactions which govern the dynamics of vegetal populations. This incorporation is achieved by adopting a mean-field idealisation which has the following advantages: though integro-differential in its formulation, it easily leads to a partial differential equation modeling the *propagation-by-reproduction* transport process specific to vegetal communities; in this form, the model can be studied by standard analytical methods and conveniently lends itself to numerical simulations, so that the dynamics it predicts can be explored in detail; though much of the complexity of natural environments is not taken into account (at least explicitly), this treatment allows us to explain the properties of TB in terms of a small (minimal) number of dimensionless parameters. In section 3, we show that the formation of vegetation patterns, and of TB in particular, is associated

[1] In the following, we encompass within the term *reproduction* the ensemble of processes corresponding to the production of seeds by the plants, the dissemination of seeds over the territory in the neighbourhood of their "mother plant," the germination of these seeds and the development of the plantules resulting from this germination into new mature plants.

with a symmetry breaking instability, the occurrence of which is not caused by the numerous sources of spatial heterogeneity (anisotropy) which natural environments unavoidably contain. This instability allows for the spontaneous formation of non-uniform vegetation density distributions even under strictly homogeneous (isotropic) conditions. Less idealised environmental conditions, such as those encountered by vegetation growing on a slope, are modeled in section 4. The results demonstrate the role that anisotropies play as a pattern selection mechanism. More particularly, we discuss the conditions under which the anisotropy associated with a surface ground slope selects an orientation of TB parallel or perpendicular to the gradient.

2. The Model.

2.1. *Assumptions.* Let $c(\mathbf{s},t)$ be the density of the vegetation at time t and point $\mathbf{s}$. We define this density as the plant biomass per unit area. The global variable $c(\mathbf{s},t)$ encompasses all vegetal species present. This is justified in all cases where vegetation patterns are formed by a one-species pure strand and where genotypic differences and age classes can be neglected. In the cases where many different species are present, we assume that those which dominate impose their spatial distribution on the others. We do not take into account explicitly the inter-species dynamics. As a place to start, we thus consider that the vegetation community reacts as a whole (Greig-Smith, 1979). The kinetic equation modeling the evolution of $c(\mathbf{s},t)$ has to express the balance between the processes contributing to the growth of the vegetation, and the processes contributing to its death or destruction. We assume that this equation is of the form

$$\partial_t c(\mathbf{s},t) = F_1 \times F_2 - F_3, \tag{1}$$

where the growth term, $F_1 \times F_2$, expresses the rate at which $c(\mathbf{s},t)$ increases. It is the product of two non-negative functions modeling two ensembles of processes which are independent insofar as they are influenced by different factors, relate to different plant structures, and operate over different spatial ranges. These processes are: in the case of F_1, the natural reproduction of plants via seed production, dissemination, germination and development into new mature plants; in the case of F_2, the interactions between plants, and between plants and the environment, which prevent the vegetation density from increasing beyond some finite upper bound or *close packed density* K. The second term on the right-hand side of equation (1) stands for vegetation spontaneous (natural) death and/or destruction by external factors such as, e.g., grazing, fire, termites, or other biological and physical agents.

Let us now define the functions F_1, F_2, and F_3. The first one, which refers to plant reproduction, we parameterise by the *replication constant* λ, the value of which depends on the number of seeds that an isolated plant produces on the average each year and on the probability that these seeds give rise to new plants when they germinate on a virgin territory. Thus, λ fixes the rate at which the density $c(\mathbf{s},t)$ increases when the interactions between plants are negligible, i.e., when their density $c(\mathbf{s},t)$ is vanishingly small. We assume that under those conditions, $c(\mathbf{s},t)$ increases exponentially with time. At high densities, when the interactions between plants can no longer be neglected, reproduction may involve *cooperative* effects: the number of seeds produced by the plants, as well as the probability that these seeds germinate and further develop, depend on the environmental conditions which may be favourably influenced by the presence of vegetation. A higher vegetation density tends to be beneficial by facilitating water percolation into the soil due to roots penetration, by decreasing water evaporation and soil crusting due to shading, and/or by increasing water collection through the accumulation of vegetal litter (Vesey-Fitzgerald, 1957). To deal with such cooperative effects, we suppose that, as the vegetation density increases, its temporal evolution becomes a non-linear function of $c(\mathbf{s},t)$. For simplicity and without important loss of generality, we take this non-linearity to be quadratic. The magnitude of this contribution is modulated by a *cooperativity parameter* Ω, having the dimensions of the inverse of a density and a value which is necessarily non-negative.

On the other hand, the variations of density taking place at a given point $\mathbf{s}$ have at least in part a *non-local* origin insofar as they result not only from the reproduction of vegetation at point $\mathbf{s}$, but also from the dissemination of seeds by the vegetation situated at neighbouring points, say $\mathbf{s}+\mathbf{s}'$. In other words, the reproduction rate at $\mathbf{s}$ integrates contributions due to the reproduction of vegetation in the neighbourhood of $\mathbf{s}$. The magnitude of these contributions depends, in general, upon the relative position of the neighbouring points $\mathbf{s}'$ considered. We express this property by introducing a weighting function $w_1 = w_1(\mathbf{s}', L_1)$ which depends on $\mathbf{s}'$ and defines the *dissemination length*, L_1, over which the neighbourhood effectively contributes to the vegetation density increase at $\mathbf{s}$. Hence, $w_1(\mathbf{s}', L_1)$ can be interpreted as giving the spatial distribution of the "daughter plants" surrounding a "mother plant" or, equivalently, as the probability of finding a "daughter plant" at point $\mathbf{s}$ when its "mother plant" is at $\mathbf{s}+\mathbf{s}'$. On the basis of these assumptions, we write F_1 as

$$F_1 = \int d\mathbf{s}'\, \lambda w_1(\mathbf{s}', L_1) c(\mathbf{s}+\mathbf{s}', t)(1+\Omega c(\mathbf{s}+\mathbf{s}', t)), \qquad (2)$$

where integration extends over the entire territory.

The function F_2 represents interactions between plants which are distinct from the cooperativity mentioned above. They inhibit vegetation reproduction and have a twofold origin. First, since each plant obviously occupies a finite surface area, $c(\mathbf{s}, t)$ can never exceed some upper physical limit, K, which we call the close packed density. Second, plants also interact in a *non-local* way, by lowering the reproduction and/or growth potentialities of plants in their neighbourhood. Therefore, in general, the carrying capacity of a territory is not constant throughout space, and simply equal to the inverse of the close packed density, i.e., K^{-1}. At any given point $\mathbf{s}$, it has an effective value which integrates the inhibitory effects that the neighbouring vegetation produces in competing for the same resources; for example, it reduces the water supply at the point considered. As in the case of F_1, we associate to this *non-local* effect a weighting function $w_2 = w_2(\mathbf{s}', L_2)$, which depends on $\mathbf{s}'$ and introduces another characteristic length distinct from L_1: the *inhibition length*, L_2, which defines the effective range over which inhibitory interactions operate. The inhibition at point $\mathbf{s}$ resulting from the vegetation present at point $\mathbf{s} + \mathbf{s}'$ can then be written as

$$\alpha \frac{w_2(\mathbf{s}', L_2)}{K} c(\mathbf{s} + \mathbf{s}', t).$$

Integrating last expression over the territory, the function F_2, which accounts for the existence of an upper bound of the vegetation density at point $\mathbf{s}$, and thus for the vanishing of the vegetation growth rate as this density is approached, is then given by

$$F_2 = 1 - \int d\mathbf{s}' w_2(\mathbf{s}', L_2) \frac{c(\mathbf{s} + \mathbf{s}', t)}{K}. \tag{3}$$

The third function in equation (1), F_3, describes the rate at which vegetation dies or is destroyed. We assume that it is proportional to the *mortality constant* η, the reciprocal of which measures the vegetation average lifetime. As before, in the case of the reproduction and inhibition functions F_1 and F_2, we suppose that the death rate F_3 may be influenced by neighbouring vegetation and we model this effect by introducing a weighting function, $w_3 = w_3(\mathbf{s}', L_3)$, which depends on $\mathbf{s}'$ and introduces another characteristic length, L_3, which we call the *toxicity length*. Accordingly, the effective death rate at the point $\mathbf{s}$,

$$F_3 = \int d\mathbf{s}' \eta w_3(\mathbf{s}', L_3) c(\mathbf{s} + \mathbf{s}', t), \tag{4}$$

is obtained by integrating the product of the vegetation density by the weighting function w_3 over the territory considered.

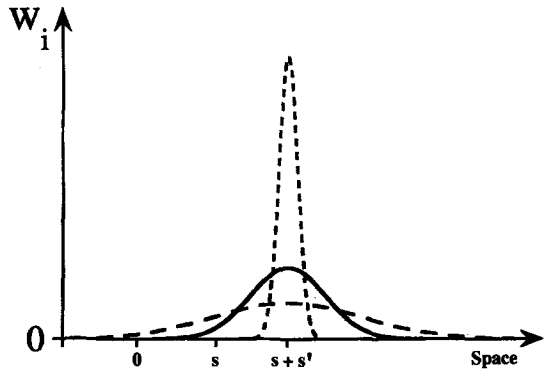

Figure 2. Sketch of the weighting functions w_i which model the non-local inter-plant interactions influencing the dynamics at s as a consequence of the presence of vegetation at a neighbouring point $\mathbf{s}+\mathbf{s}'$. The range of toxic interactions influencing plant mortality, L_3 (weighting function w_3, short dashes), is small compared to the reproduction range L_1 (weighting function w_1, full line) and inhibition range L_2 (weighting function w_2, long dashes). All w_i's are decreasing functions of the distance between interacting points; the environment is supposed to be isotropic.

2.2. *Properties of the weighting functions.* Replacing expressions (2), (3), (4) in equation (1) yields that the vegetation density $c(\mathbf{s},t)$ obeys the following kinetic equation:

$$\partial_t c(\mathbf{s},t) = \left[\int d\mathbf{s}'\, \lambda w_1(\mathbf{s}', L_1) c(\mathbf{s}+\mathbf{s}', t)(1+\Omega c(\mathbf{s}+\mathbf{s}', t))\right] \cdot\left[1 - \int d\mathbf{s}'\, w_2(\mathbf{s}', L_2)\, \frac{c(\mathbf{s}+\mathbf{s}', t)}{K}\right] - \int d\mathbf{s}'\, \eta w_3(\mathbf{s}', L_3) c(\mathbf{s}+\mathbf{s}', t). \tag{5}$$

For this model to be complete, the weighting functions w_i $(i = 1,2,3)$ must still be specified. By choosing these functions, the properties of particular vegetation and/or territories can be fitted. The mathematical form of the w_i's is thus system-dependent and cannot be fixed once and for all. There are, however, several important properties, illustrated in Fig. 2, which these functions should possess in general:

(i) They should be non-negative everywhere:

$$w_i = w_i(\mathbf{s}', L_i) \geq 0, \qquad \forall \mathbf{s}'. \tag{6}$$

(ii) For systems exhibiting no direction of anisotropy (e.g., a slope imposing to rainwater a well-defined running down direction), they should be invariant w.r.t. the operation of rotation; their variation

should then only depend on the distance $s' \equiv |\mathbf{s}'|$ separating the points between which the interactions are evaluated. Furthermore, the w_i's should be maximum at $s' = 0$, monotonously decreasing with s', and tending to zero as s' tends to infinity. Their range L_i should simply represent the distance beyond which non-local effects become negligible.

(iii) When the interaction ranges L_i tend to zero, for isotropic systems, the dynamics becomes *strictly local*. The weighting functions $w_i(\mathbf{s}', L_i)$ should then reduce to δ distributions,

$$\lim_{L_i \to 0} w_i(\mathbf{s}', L_i) = \delta(\mathbf{s}'), \tag{7}$$

implying that the kinetic equation (5) transforms into a standard Verhulst-Fisher type of equation (Fife, 1979),

$$\partial_t c(\mathbf{s}, t) = [\lambda c(\mathbf{s}, t)(1 + \Omega c(\mathbf{s}, t))]\left[1 - \frac{c(\mathbf{s}, t)}{K}\right] - \eta c(\mathbf{s}, t),$$

describing the evolution of a population deprived of any mean of spatial propagation.[2]

(iv) The $w_i(\mathbf{s}', L_i)$'s must be normalised:

$$\int d\mathbf{s}' \, w_i(\mathbf{s}', L_i) = 1. \tag{8}$$

This condition simply expresses that all interactions generated on the territory necessarily end up somewhere on the territory.

For isotropic environments, we take as weighting functions w_i's the gaussian distribution functions:

$$w_i(\mathbf{s}', L_i) = \frac{1}{(2\pi)^{d/2} L_i^d} \, e^{-(|\mathbf{s}'|^2 / 2L_i^2)}, \tag{9}$$

where d corresponds to the space-dimension (2 in the present context). This choice satisfies conditions (i)–(iv) above and seems justified qualitatively, for many vegetal populations. At the same time, it avoids mathematical complexities which are not essential for the general purpose, which is ours, of discussing those aspects of vegetation patterns which do not specifically depend on the nature of the plants and soils involved. Our aim in the next section is to determine the conditions under which these patterns can form as a result of non-local interactions such as those

[2] For vanishing death rate, i.e., when $\eta = 0$, the density $c(\mathbf{s}, t)$ simply grows monotonously in time until it reaches the close packed density K.

described by expressions (2), (3), (4). We will see that their appearance depends fundamentally upon the existence of well-defined relationships between the interaction ranges L_i.

3. Symmetry Breaking and Pattern Formation under Spatially Isotropic Environmental Conditions. Many environmental constraints have a spatial structure. As a result, the processes influenced by these constraints, instead of occurring in a spatially isotropic manner, become spatially oriented. Dominant winds, for instance, influence seed dissemination and may enhance plant reproduction in the downwind direction[3]; similarly, on a sloping territory rainwater streaming creates an anisotropy in the distribution of seed germination spots and thus favours the propagation of vegetation in a particular direction.[4] We shall see in section 4 that such spatial anisotropies of external origin play a determinant role in *pattern selection mechanisms*, e.g., they select how the stripes of TB are oriented on the territory.

These external anisotropies, however, are unlikely to be the cause of the phenomenon itself. It is hard to see how they could give rise to such systematic and well-defined regularities as those displayed by TB. It is much more likely that the latter arise by a self-regulatory dynamical mechanism capable of generating periodic vegetation distributions even in isotropic environments.

To start with, let us try to guess the dynamical factors which explain the organisation of plant communities in arid regions. Reasoning as Clos-Arceduc (1964), we consider the fate of a plant which needs a minimal quantity of water to survive. For a fixed annual rainfall, this quantity corresponds to a minimal ground area which the plant root system pumps dry. As the climate gets more arid, the annual rainfall decreases. To compensate, the plant needs to have an increased drainage area at its disposal. But if this area becomes greater than that protected by its foliage against the sun and dry wind, which are the main factors responsible for evaporation, the plant either dies, if it is isolated, or perhaps survives if it is surrounded by other plants and benefits from an increased protection against evaporation procured by the foliage of the latter. In this interpretation, vegetation clustering is viewed as a natural response to more arid environmental conditions. There are, however, obvious limitations to this (cooperative) protective clustering effect. For example, if the resources (especially water) of the plants growing inside a cluster are mostly consumed by neighbouring plants, the central plants will again die without

[3] Wind may also have an inhibitory or even mortal effect on the vegetation due to defoliation (Ives, 1946; Moloney, 1986).

[4] Slopes may, of course, also have an inhibitory effect on the vegetation due to the redistribution of water they imply.

replacement, this time not as a result of evaporation, but due to some *inhibitory effect* of the vegetal population on itself. This suggests that the wavelength of TB is a compromise between two spatial scales: one characterising the cooperative reproduction of the population; the other characterising the self-inhibition effects through which the population hampers its own growth.

The mechanism proposed below translates these intuitive ideas in mathematical terms. It attributes the formation of vegetation patterns to a symmetry breaking instability which homogeneous vegetation distributions may undergo even if the environmental conditions are strictly isotropic. Typically, this instability triggers the appearance of spatial inhomogeneities the characteristic length of which is determined by the ranges L_i characterising the interactions existing inside the vegetation community. The latter, rather than some anisotropic external constraint or boundary condition, appear to be the governing parameters of the population spatial organization.

It is thus best to discuss at first the mechanism of this instability for the idealised conditions of a territory subjected to strictly isotropic environmental constraints. This is the purpose of this section. The more complex situation of an anisotropic environment will be dealt with in section 4.

3.1. *Uniform steady state distributions.* Using the expressions (9) for the weighting functions, normalising time, space and density by setting

$$\{\tau, \mathbf{r}, \rho(\mathbf{r},\tau)\} \equiv \left\{\lambda t, \frac{\mathbf{s}}{L_2}, \frac{c(\mathbf{s},t)}{K}\right\}, \tag{10}$$

and defining the dimensionless combinations of parameters

$$\{\Lambda, \mu, L, L'\} \equiv \left\{K\Omega, \frac{\eta}{\lambda}, \frac{L_1}{L_2}, \frac{L_3}{L_2}\right\}, \tag{11}$$

the kinetic equation (5) can be rewritten in dimensionless form as ($d = 2$)

$$\begin{aligned}\partial_\tau \rho(\mathbf{r},\tau) = &\left[\frac{1}{2\pi L^2}\int d\mathbf{r}'\, e^{-(|\mathbf{r}'|^2/2L^2)}\rho(\mathbf{r}+\mathbf{r}',\tau)(1+\Lambda\rho(\mathbf{r}+\mathbf{r}',\tau))\right]\\ &\cdot\left[1-\frac{1}{2\pi}\int d\mathbf{r}'\, e^{-(|\mathbf{r}'|^2/2)}\rho(\mathbf{r}+\mathbf{r}',\tau)\right]\\ &-\frac{\mu}{2\pi L'^2}\int d\mathbf{r}'\, e^{-(|\mathbf{r}'|^2/2L'^2)}\rho(\mathbf{r}+\mathbf{r}',\tau).\end{aligned} \tag{12}$$

It admits two uniform steady state branches of solutions:

$$\rho_0 = 0 \quad \text{and} \quad \rho_\pm = \frac{\Lambda - 1 \pm \sqrt{(\Lambda - 1)^2 + 4\Lambda(1 - \mu)}}{2\Lambda}. \tag{13}$$

The first one, ρ_0, represents a territory deprived of any vegetation; obviously it exists for all values of the parameters. The second one, $\rho_\pm$, has to be real and non-negative to represent a vegetation density; in fact, the values of $\rho_\pm$ belong to the interval $[0, 1]$, since the close packing density K is normalised to 1 by the change of variables (10). Two cases must then be distinguished according to whether the parameter Λ measuring the cooperative effects influencing reproduction is less or greater than 1 (see Fig. 3).

In the first case,

$$\Lambda \leq 1 \quad \text{and} \quad 0 \leq \mu \leq 1, \tag{14}$$

cooperativity is weak and there exists, for each value of μ in the interval $[0, 1]$, a unique non-zero homogeneous steady state, given by ρ_+. It is maximum and equal to 1 for $\mu = 0$. As μ increases, the steady state branch ρ_+ monotonously decreases till the switching point $\mu = 1$ is reached. At this point, the probability of reproduction of an isolated plant becomes less

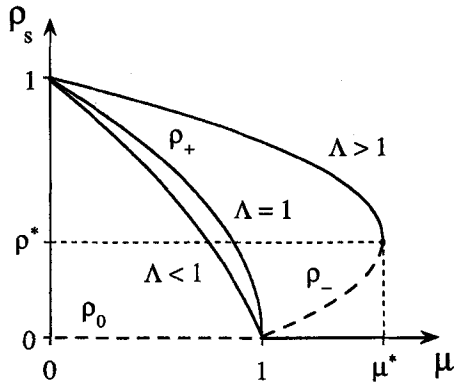

Figure 3. Uniform steady state solutions and their stability w.r.t. homogeneous perturbations (corresponding to $k = 0$, cf. subsection 3.2). The vegetation-free steady state, $\rho_0 = 0$, is always a solution of the kinetic equation; it is unstable (dashed line) for $0 \leq \mu < 1$ and stable otherwise. Depending upon whether Λ is less or greater than 1, the steady state branch of solutions $\rho_\pm$ exhibits a hysteresis loop. Clearly, cooperative interactions allow vegetation to survive under harsher environmental conditions. For $\Lambda \leq 1$ and $\mu > 1$, or $\Lambda > 1$ and $\mu > \mu^*$, the only stable state is ρ_0 (full line). For $\Lambda > 1$ and $1 \leq \mu \leq \mu^*$, ρ_- exists and is unstable (dashed line); for $\Lambda \leq 1$ and $0 \leq \mu \leq 1$ or $\Lambda > 1$ and $0 \leq \mu \leq \mu^*$, ρ_+ is stable (full line). The density $\rho^* = (\Lambda - 1)/2\Lambda$ is the boundary between ρ_+ and ρ_-.

than its probability of death; accordingly, the steady state branch ρ_+ intersects the trivial branch ρ_0, i.e., vanishes. In the following, we shall therefore call μ the *switching parameter.*[5] When $\mu > 1$, no real non-negative solution exists: the survival of vegetation is impossible.

In the second case,

$$\Lambda > 1 \quad \text{and} \quad 0 \leq \mu \leq \frac{(1+\Lambda)^2}{4\Lambda} \equiv \mu^* \qquad (\mu^* > 1), \tag{15}$$

cooperativity is strong. As a result, the steady state branch of solutions $\rho_\pm$ exhibits a hysteresis loop in the range $1 \leqslant \mu \leqslant \mu^*$. Thanks to the fact that plants mutually protect each other, non-zero uniform steady state densities ρ_+ and ρ_- can be observed, for values of μ greater than 1.

3.2. *Symmetry breaking instability.* We look for conditions under which the establishment of a uniform vegetation distribution is impossible because the non-zero homogeneous steady state branch of solutions ρ_+ is unstable w.r.t. a finite band of spatial modes. This unstable band must exclude both the very large wavelengths (small wave numbers), corresponding to quasi-uniform vegetation distributions, and the very short wavelengths (large wave numbers), corresponding to inhomogeneities varying in space much more quickly than the interactions. This Turing-kind of symmetry breaking scenario is well known to entail the formation of a pattern the periodicity of which is determined by the intrinsic parameters governing the dynamics rather than by geometrical factors and/or boundary conditions (Turing, 1952; Cross and Hohenberg, 1993).

Before examining the stability properties of the $\rho_\pm$ branch of solutions, it is useful to investigate the linear stability of the trivial steady state ρ_0 and to show that to be consistent with the mean-field treatment adopted here, the condition $L_1 > L_3$ must be satisfied. Writing that an arbitrary deviation $\delta\rho(\mathbf{r}, \tau)$ from the reference state ρ_0 is given in Fourier space by

$$\delta\rho(\mathbf{r}, \tau) = \frac{1}{2\pi} \int \mathrm{d}\mathbf{k}\, \delta\tilde{\rho}(\mathbf{k}, \tau) \mathrm{e}^{i\mathbf{k}\cdot\mathbf{r}}, \tag{16}$$

where $\delta\tilde{\rho}(\mathbf{k}, \tau) = \mathrm{e}^{\omega_k \tau}\, \delta\tilde{\rho}(\mathbf{k}, 0)$ is the amplitude associated to the wave vector $\mathbf{k}$, replacing expression (16) in equation (12) and retaining only linear terms,

[5] In this context, μ could also be interpreted appropriately as a parameter measuring the aridity of the territory considered.

we easily obtain that the eigenvalue ω_k associated to the wave vectors of modulus $k \equiv |\mathbf{k}|$ is given by

$$\omega_k = e^{-(L^2k^2/2)} - \mu e^{-(L'^2k^2/2)}. \tag{17}$$

In agreement with the notion that (isolated) plants cannot survive if the switching parameter μ (death-to-birth ratio) exceeds 1, relation (17) shows that ρ_0 is stable (unstable) w.r.t. the homogeneous mode $k = 0$, when $\mu > 1$ ($0 \leq \mu < 1$).

On the other hand, since the integrals appearing in equation (12) average out inhomogeneities the wavelengths of which are much smaller than the interaction lengths L_i, it is consistent with the coarse-graining treatment adopted here to require that, whatever the value of μ, all modes corresponding to wave numbers k larger than some upper cut-off value k_u are stable: ρ_0 should be stable for k tending to infinity, or alternatively w.r.t. inhomogeneities the wavelengths of which tend to zero. In Appendix A, we show that this condition amounts to asking that the inequality $L > L'$ holds, i.e., that the cooperative dissemination length L_1 exceeds the toxicity length L_3:

$$L_1 > L_3. \tag{18}$$

Henceforth, we shall suppose that inequality (18) is amply satisfied. It is indeed plausible that compared to reproduction, which involves the process of seed dissemination, vegetation death is a short-ranged, essentially local process. For simplicity and without important loss of generality, we shall therefore set $L_3 = 0$ ($L' = 0$) in the following.

We now investigate the linear stability of the $\rho_\pm$ uniform steady state branch of solutions. The eigenvalue associated to the kth Fourier mode is in that case given by

$$\omega_k = (1 - \rho_s)(1 + 2\Lambda\rho_s)e^{-(L^2k^2/2)} - \rho_s(1 + \Lambda\rho_s)e^{-(k^2/2)} - (1 - \rho_s)(1 + \Lambda\rho_s), \tag{19}$$

where the values of $\rho_s \equiv \rho_\pm$ belong to the interval $[0, 1]$. The behaviour of this eigenvalue summarises as follows. The rapidly varying inhomogeneous modes are always stable: in the limit k going to infinity, the eigenvalue ω_k is always negative; one simply has $-(1 - \rho_s)(1 + \Lambda\rho_s)$. As already noted above, this is consistent with the coarse-grained treatment adopted to describe the interactions existing within the vegetal community. When the vegetation is close packed ($\rho_s = 1$, $\mu = 0$), the uniform distribution is stable w.r.t. perturbations of any wave number k. If ρ_s exhibits no hysteresis loop (i.e., when $\Lambda \leq 1$), the vegetation density tends necessarily to 0 when the

switching parameter μ tends to 1: the environmental conditions getting more arid, the vegetation becomes extinct. In this limit, the eigenvalue ω_k tends to $\exp(-L^2k^2/2)-1$, and clearly the uniform distribution ρ_s is stable: the plants are getting thinly dispersed over the territory so that their interactions become negligible and thus, in first approximation, each plant behaves as if it were isolated. If ρ_s exhibits a hysteresis loop (i.e., when $\Lambda > 1$), the homogeneous mode $k=0$ is stable (unstable) for $\rho_s = \rho_+$ ($\rho_s = \rho_-$). Finally, we note that if there exists a wave number $k = k_c > 0$ for which the conditions

$$(\omega_k)_{k=k_c} = 0, \qquad \left(\frac{d\omega_k}{dk}\right)_{k=k_c} = 0, \qquad \left(\frac{d^2\omega_k}{dk^2}\right)_{k=k_c} < 0, \tag{20}$$

can be fulfilled for positive values of the parameters, the stability of the steady state ρ_+ becomes marginal. This value of k_c, which marks the appearance of a finite band of unstable modes and hence of a symmetry breaking instability, can be calculated from the first two of these conditions. One obtains

$$k_c = \sqrt{\frac{2}{L^2-1}\ln\left[\frac{(1-\rho_c)(1+2\Lambda\rho_c)L^2}{\rho_c(1+\Lambda\rho_c)}\right]}, \tag{21}$$

where ρ_c is solution of

$$-(1+\Lambda\rho_c)+(1-L^2)(1+2\Lambda\rho_c)\left[\frac{(1-\rho_c)(1+2\Lambda\rho_c)L^2}{\rho_c(1+\Lambda\rho_c)}\right]^{L^2/(1-L^2)} = 0, \tag{22}$$

and belongs to the interval $]0,1[$.

Two interesting results can immediately be derived from equation (22) by looking for the conditions under which it admits physically acceptable solutions. First, one sees that the occurrence of the symmetry breaking instability requires that *the self-inhibition length must be greater than the dissemination length*,[6]

$$L < 1, \quad \text{or equivalently that} \quad L_1 < L_2. \tag{23}$$

Second, one sees that *the reproduction process must be cooperative*, i.e., that one must have

$$\Lambda > 0. \tag{24}$$

[6] This condition is the analogue of the short-range activation–long-range inhibition condition typical of Turing instabilities in reaction-diffusion systems.

Indeed, for $\Lambda = 0$ and thus $\rho_c = 1 - \mu_c$, relation (21) reads

$$k_c = \sqrt{\frac{2}{L^2 - 1} \ln\left[\frac{\mu_c}{1 - \mu_c} L^2\right]}, \tag{25}$$

while equation (22) reduces to

$$-1 + (1 - L^2)\left[\frac{\mu_c}{1 - \mu_c} L^2\right]^{L^2/(1-L^2)} = 0. \tag{26}$$

Clearly, in order that equation (26) admits a solution, it is necessary that $L < 1$, and thus that $\mu_c L^2/(1 - \mu_c) < 1$, in order that relation (25) be real, which turns out to be incompatible with the existence of an acceptable solution for equation (26).

The mechanism of appearance of a finite band of unstable modes, from which the homogeneous mode $k = 0$ is excluded and which thus entails the occurrence of a symmetry breaking instability, is represented in Fig. 4. In Fig. 4a, one sees that unstable modes appear as soon as $L < L_c$ ($\Lambda > 0$, and

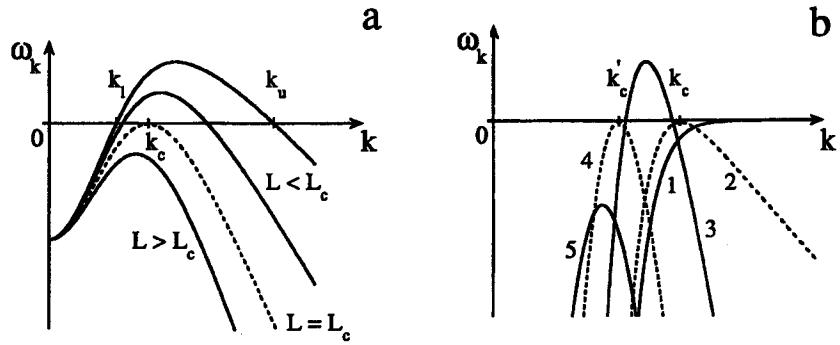

Figure 4. (a) Sketch of the eigenvalues ω_k as a function of the wave number k for different values of L. When L decreases, a finite range of unstable modes appears. When $L > L_c$, all modes are stable; $L = L_c$ is the critical value for which a real eigenvalue changes sign for $k = k_c$ (dashed line); when $L < L_c$, the modes between k_l and k_u are unstable. Vanishingly small wave numbers and arbitrarily large wave numbers are always stable. (b) Sketch of the behaviour of the eigenvalues ω_k as a function of the wave number k for different values of μ when $\Lambda \leq 1$. When μ is close to 0, the homogeneous stationary density $\rho_s = \rho_+$ approaches 1; no symmetry breaking instability is then possible. When μ approaches 1, ρ_s becomes close to 0 where no instability is possible either. So that when μ increases from 0 to 1, the succession stability-instability-stability is as follows: first, all modes are stable for $\mu < \mu_c$ (curve 1); second, there appears a critical mode k_c for $\mu = \mu_c$ (curve 2), so that when $\mu_c < \mu < \mu'_c$ (curve 3), there exists a finite interval of unstable modes; third, there appears a second critical mode k'_c for $\mu = \mu'_c$ (curve 4), so that when $\mu > \mu'_c$ (curve 5), all modes are stable again.

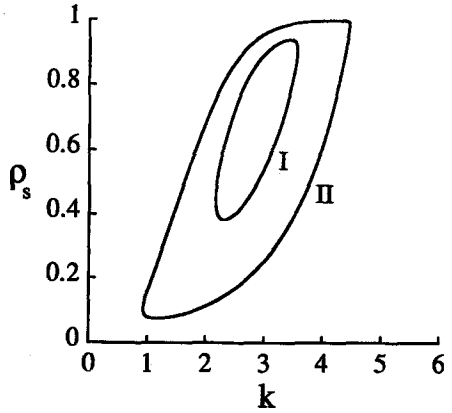

Figure 5. The intervals of unstable modes are shown in terms of the local steady state density $\rho_s = \rho_+$ for $\Lambda = 0.5$ (I) and $\Lambda = 1$ (II); L being fixed at 0.2. The unstable modes are enclosed by the curves. The domain of instability increases with Λ, showing that cooperativity of the reproduction process favours the occurrence of the patterning phenomenon. One notes that the interval of unstable modes shifts toward smaller k's for decreasing values of ρ_s, predicting, in agreement with field observations, that the wavelength of the vegetation patterns increases under more arid conditions.

μ being kept fixed). For values of L decreasing further, the width of the unstable band gets broader both on the side of the large wave numbers and on the side of the small wave numbers: the band lower cut-off k_l decreases, while simultaneously its upper cut-off k_u increases. On the other hand, the wave number of the fastest growing mode, which determines the characteristic length of the pattern appearing for L inferior but close to L_c, progressively drifts towards larger values (smaller wavelengths). Figure 4(b) shows how the unstable modes behave as μ increases ($L < 1$ and $0 < \Lambda \leq 1$ being kept fixed). Given that for $\rho_s = \rho_+ = 1$, or equivalently for $\mu = 0$, the system is stable, the marginal stability point (20) is reached by increasing the switching parameter μ up to some finite value $\mu = \mu_c > 0$. Beyond this point, a further increase of the switching parameter induces the appearance of a finite band of unstable modes. There exists, however, an upper critical value $\mu = \mu_c' > 0$ beyond which the homogeneous steady state branch ρ_+ becomes stable again. Indeed, the domain of instability excludes both the points[7] $\mu = 0$ and $\mu = 1$ when $\Lambda \leq 1$ (cf. above). When $\Lambda > 1$, the values of μ for which ρ_+ is unstable may extend up to $\mu = \mu^*$ (see Fig. 3).

The conditions for a symmetry breaking instability are further illustrated in Fig. 5. The instability domain, corresponding to the areas enclosed by the curves, has been represented in the (k, ρ_s)-space for two values of the cooperativity Λ and for a fixed value of L. One notes that as the environment gets more arid, i.e., when ρ_s decreases, the modes k_l and k_u shift

[7] In general, some finite neighbourhood of these points.

towards the small wave numbers (large wavelengths). This suggests, in agreement with *in situ* observations, that the width of the vegetation bands should increase under those conditions. This behaviour finally leads to the disappearance of the instability when ρ_s tends to 0.

We shall see in section 3.4 that the instability leads in isotropic environments to the formation of patterns having a roll-type or hexagonal symmetry.

3.3. *Approximation of the model by a partial differential equation.* Equation (12) is an integro-differential equation which has the advantage of being compact. It is, however, not of easy use for undertaking an analytical investigation of its non-linear behaviours when the uniform steady states ρ_s becomes unstable; it is also not a convenient starting point for implementing a numerical exploration of these non-linear solutions. This requires the discretisation of the integrals appearing in equation (12), which is prohibitive in terms of computer time. Therefore, we prefer to deal with this problem by using a partial-differential-equation approximation of equation (12). We obtain the latter by expanding the vegetation densities $\rho(\mathbf{r}+\mathbf{r}', \tau)$ in Taylor series (Murray, 1993),

$$\rho(\mathbf{r}+\mathbf{r}', \tau) = \sum_{n=0}^{\infty} \frac{1}{n!}(\mathbf{r}' \cdot \nabla)^n \rho(\mathbf{r}, \tau). \tag{27}$$

As explained in Appendix B, fourth-order terms must be retained in this expansion in order that the linear stability properties of the partial-differential and integro-differential versions of the model be qualitatively identical. The fourth-order differential terms are stabilising; they guarantee the existence of an upper cut-off on the band of unstable modes. The situation is reminiscent of the mean-field treatment of spinodal decomposition based on the Cahn and Hilliard equation, where the instability associated with the appearance of a negative diffusion coefficient is controlled by including fourth-order differential terms modeling surface tension effects (see, e.g., Gunton *et al.*, 1983; Langer, 1992). We obtain the desired approximation in the form

$$\begin{aligned}\partial_\tau \rho(\mathbf{r}, \tau) = &\left[\left(1 + \tfrac{1}{2}L^2\nabla^2\right)(\rho(\mathbf{r}, \tau)(1 + \Lambda\rho(\mathbf{r}, \tau)))\right]\left[1 - \left(1 + \tfrac{1}{2}\nabla^2\right)\rho(\mathbf{r}, \tau)\right] \\ &- \tfrac{1}{8}\rho(\mathbf{r}, \tau)(1 + \Lambda\rho(\mathbf{r}, \tau))\nabla^4\rho(\mathbf{r}, \tau) - \mu\rho(\mathbf{r}, \tau).\end{aligned} \tag{28}$$

3.4. *Numerical simulations.* The results reported below are obtained by integrating equation (28) numerically. The integration domain corresponds to a square-shaped territory subjected to periodic boundary conditions. The initial condition is chosen to be an unstable uniform steady state density ρ_+

perturbed by some small-amplitude random noise. This noise stands for the numerous more or less random environmental factors which disturb the uniformity of natural mediums, e.g., ant or termite activity, which is both benefic (nests increase water infiltration by soils) and detrimental (eroded material from nests increases runoff) to vegetation (Ouedraogo and Lepage, 1996), fire or grazing, vegetal debris, animal excreta accumulations,... (Boaler and Hodge, 1964; Hemming, 1965; White, 1971).

In the course of time, the system evolves towards a stationary and spatially periodic pattern the symmetry properties of which depend on the value of the parameters kept fixed. Figure 6 reports three types of regular spatial structures obtained for different values of the parameters μ, Λ and L. The first two patterns are of the roll-type: they are constituted of an alternation of densely and weakly populated vegetation bands; the width of these bands is approximately equal to $\lambda_c = 2\pi/k_c$. This result confirms that even under isotropic environmental conditions, vegetation stripes are possible: homogeneous, flat territories can support tiger bush formations.

This prediction of the model steps aside from the rather general opinion that the existence of a ground slope is necessarily involved in the formation of TB (Greenwood, 1957; Worrall, 1959; Greig-Smith, 1979). Interestingly, we may emphasize that as such, the model is able to explain the existence of banded patterns, which has been reported on virtually levelled grounds (Clos-Arceduc, 1956; White, 1969), and thus that it is not necessary, in order to explain these observations, to invoke, as some authors do, the presence of neighbouring declivities. The plausibility of this latter interpretation can be further questioned in view of the fact that the width and the regular spacing of the bands far from the edge of these declivities cannot

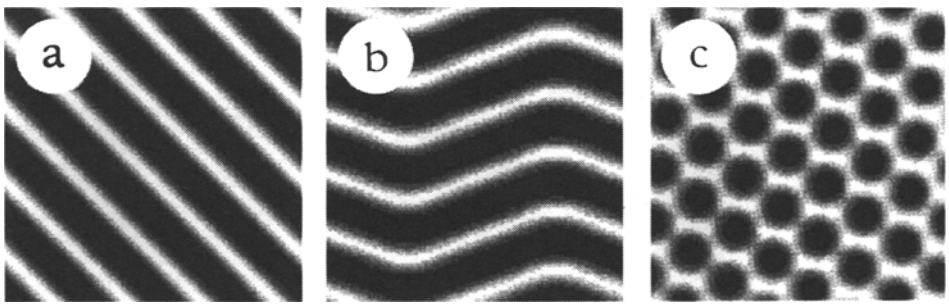

Figure 6. Three examples of spatial patterns obtained for an isotropic system (white regions correspond to less vegetated areas). (a) Pattern constituted of stripes having a uniform orientation ($\mu = 0.95$, $L = 0.1$, $\Lambda = 1$). The latter is determined by the initial condition. (b) Coexistence of stripes with two different orientations ($\mu = 0.95$, $L = 0.15$, $\Lambda = 1$). The relative orientation is determined by the choice of the parameters, while the global orientation is again only dependent on the initial condition. (c) High-density spots arranged in hexagonal lattice on a low-density background ($\mu = 0.95$, $L = 0.1$, $\Lambda = 0.8$). In all cases, the periodicity corresponds to a wavelength approximately given by $\lambda_c = 2\pi/k_c$.

be understood by a water flowing-absorption equilibrium (Litchfield and Mabbutt, 1962; Galle and Seghieri, 1994): it is indeed unlikely that water running down from the escarpments would cross more than one or two densely vegetated bands (Cornet *et al.*, 1988).

Let us remark also that the relation between vegetation cover and microrelief is unclear. In Niger, the mean ground slope can be higher in the bare interbands than in the vegetated bands (Ehrmann *et al.*, 1996), whereas in Australia, the opposite situation is observed: unvegetated bands have a lower gradient than grassed bands (Dunkerley and Brown, 1996). Moreover, the idea that the local topography could determine the spatial organisation of vegetation has been questioned recently, in particular by Audry and Rossetti (1996). According to these authors, in Mauritania, it is the existence of vegetation bands themselves which, in the first place, creates differences in the microtopography, rather than the microtopography which causes the formation of bands. On a more global scale, the role of ground slopes seems clearer. Plains, with no consistent slope, often bear a vegetation distribution consisting of scattered clusters of trees and shrubs, while grounds with a significant mean gradient usually support vegetation organised in bands (Couteron, 1996) oriented orthogonally to the direction of the ground slope. These observations suggest that the pattern spatial symmetry depends on the overall ground slope in a consistent manner: banded patterns, oriented at right angle to the slope, being generally preferred over spotted ones. We shall come back to this selection problem in section 4, where we model the effects of environmental anisotropies.

In Fig. 6a, the orientation of the stripes is determined by the random initial condition. Clusters of specific size, approximately given by $\lambda = 2\pi/k_c$, appear in the early stage of the evolution and subsequently, on a long time scale, finally merge with each other to form the final banded ordered state. We plan to study in detail in a forthcoming publication the different transient dynamical regimes involved in this evolution. In the final state, the orientation of the bands is stable w.r.t. small-amplitude random fluctuations: no spatial direction or position is privileged (the Fourier transform of the fluctuations is essentially constant). In Fig. 6b, there are two distinct directions whose relative orientation depends on the dynamics, while their orientation as a whole is again determined at random by the initial condition. This exemplifies that, as expected, under isotropic environmental conditions, the dynamics involves no mechanism capable of selecting a particular orientation of the patterns.

Figure 6c consists of higher-density spots distributed on a hexagonal lattice. The distance between two neighbouring spots is roughly given by λ_c. It corresponds to vegetation clusters of fixed size, equally spaced, surrounded by a less densely vegetated background. To our knowledge, no vegetation pattern possessing this kind of spatial symmetry has, up to now, been described in arid or semi-arid regions. Three possible reasons may

explain this lack: (i) It is more difficult to detect a hexagonal symmetry than a linear one in vegetation patterns, which are generally perturbed by random irregularities. (ii) The presence of an environmental anisotropy, such as a slope of the terrain or the prevailing wind direction, can plausibly destabilise a hexagonal structure and select instead a roll-type one. (iii) In the isotropic case, the vegetation is obviously less inhibited by neighbours on the system border. Therefore, the latter could be the starting point of an inward patterning wave, leaving behind an alternation of more and less dense lines of vegetation parallel to the system edge (Clos-Arceduc, 1964).

The second of these putative reasons is further studied in the next section by modeling the effect of anisotropic weighting functions on the dynamics.

4. Symmetry Breaking Conditions on Anisotropic Territories. Anisotropic environmental conditions are common and can be grouped into two classes: (i) Atmospherical factors such as wind and light. The sun trajectory in the sky may induce a shadow direction so that one side of the vegetation is receiving more light than the other. (ii) Geomorphological factors such as ground surface and structure. On terrains which exhibit a slope, the soil is generally more compact downslope than upslope because of gravitational effects (Ruxton and Berry, 1960; Glover *et al.*, 1964; White, 1971).

Among the various anisotropies which are encountered, one may distinguish those which conserve the $\mathbf{r} \leftrightarrow -\mathbf{r}$ invariance from those which do not. The first kind can select the spatial symmetry of the pattern and its orientation, but the pattern remains static. The second kind can, in addition to the pattern selection capabilities of the first, induce a global movement of the pattern.

The regular vegetation patterns observed in arid regions consist either of stripes running parallel to the ground slope or of sinuous bands and arcs the main axis of which is orthogonal to the ground slope (Boaler and Hodge, 1962 and 1964). In the latter case, often an upslope migration at a speed proportional to the reproduction rate of the vegetal species takes place. This has been observed, notably with herbs and grasses ($\lambda^{-1} \sim$ year) (Worrall, 1959), and deduced from indirect measurement in the case of shrubs and trees ($\lambda^{-1} \sim$ century) (Cornet *et al.*, 1988; Montaña *et al.*, 1990).

Anisotropy must be introduced in the model at the level of the weighting functions and break their $\mathbf{r} \leftrightarrow -\mathbf{r}$ symmetry. The simplest way of achieving this is by translating the weighting functions w_i of an oriented distance d_i in a given direction, say y (the positivity and normalisation properties of the weighting functions obviously hold under such a displacement). Taking, as before, the limit L' going to 0 (vegetation death is considered to be a

local process), equation (12) then reads

$$\partial_\tau \rho(\mathbf{r},\tau) = \left[\frac{1}{2\pi L^2}\int d\mathbf{r}'\, e^{-\{[x'^2+(y'-t_1)^2]/2L^2\}}\rho(\mathbf{r}+\mathbf{r}',\tau)(1+\Lambda\rho(\mathbf{r}+\mathbf{r}',\tau))\right]$$
$$\cdot\left[1-\frac{1}{2\pi}\int d\mathbf{r}'\, e^{-\{[x'^2+(y'-t_2)^2]/2\}}\rho(\mathbf{r}+\mathbf{r}',\tau)\right]-\mu\rho(\mathbf{r},\tau), \quad (29)$$

where t_i $(i=1,2)$ are two new dimensionless parameters which describe the magnitude of the displacement d_i in units of the *inhibition length* L_2:

$$t_i = \frac{d_i}{L_2}. \quad (30)$$

Positive (negative) values of t_1 correspond to situations where the plants reproduce preferentially in the positive (negative) y direction; positive (negative) values of t_2 correspond to situations where the plants inhibit more their neighbours in the positive (negative) y direction.

The homogeneous steady states are unchanged, but their linear stability with respect to inhomogeneous perturbations now obeys the dispersion relation

$$\begin{aligned}\omega_{\mathbf{k}} = &-\mu+(1-\rho_s)(1+2\Lambda\rho_s)\cos(t_1k_y)e^{-(L^2|\mathbf{k}|^2/2)}\\ &-\rho_s(1+\Lambda\rho_s)\cos(t_2k_y)e^{-(|\mathbf{k}|^2/2)}\\ &+i\left[(1-\rho_s)(1+2\Lambda\rho_s)\sin(t_1k_y)e^{-(L^2|\mathbf{k}|^2/2)}\right.\\ &\left.-\rho_s(1+\Lambda\rho_s)\sin(t_2k_y)e^{-(|\mathbf{k}|^2/2)}\right]. \quad (31)\end{aligned}$$

The eigenvalues (31) associated to the Fourier modes have now an imaginary part, consequence of the broken symmetry $\mathbf{r}\leftrightarrow-\mathbf{r}$. This property allows for the appearance of traveling patterns.

The stability properties of the system, in particular the critical wave number of the first mode which becomes unstable, are fully determined by $Re\,\omega_{\mathbf{k}}$. One sees that[8]: as in the isotropic case, the maximum density $\rho_s=1$ ($\mu=0$) is always stable; small wavelengths corresponding to large values of $|\mathbf{k}|$ are stable at all densities; the wave vector $\mathbf{k}=0$ is (un)stable for $\rho_s=\rho_{(-)+}$ and (un)stable for $\rho_s=0$ when $\mu(>)<1$. Furthermore, the real part of the dispersion relation is invariant under the transformations $t_i\to-t_i$, while the imaginary part changes sign. This means that the sign of the parameters t_i can only affect the motion of the spatial pattern.

Qualitatively, the influence of anisotropy on $Re\,\omega_{\mathbf{k}}$ is best seen by considering separately the two cases $t_1\neq0$, $t_2=0$ and $t_1=0$, $t_2\neq0$ illus-

[8] Subject to the conditions $|t_ik_y|<\pi/2$ $(i=1,2)$ which assure the positivity of the cosine factors and avoid artefacts due to the ansatz employed to model anisotropy.

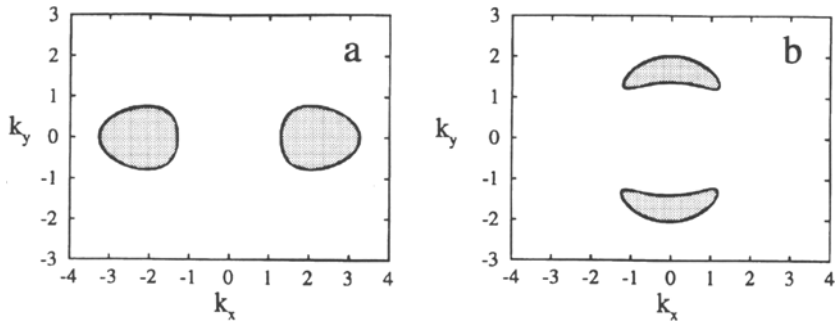

Figure 7. Two independent behaviours of $\omega_{\mathbf{k}}$ in the anisotropic case. (a) When the anisotropy in the y direction is acting only upon reproduction ($\mu = 0.9$, $L = 0.2$, $\Lambda = 1$, $t_1 = 0.5$ and $t_2 = 0$), the unstable wave vectors (shaded regions) are preferentially aligned in the k_x direction, giving rise to stripes parallel to the y direction, at least in the early stage of the evolution. (b) When the anisotropy affects only inhibition ($\mu = 0.9$, $L = 0.3$, $\Lambda = 1$, $t_1 = 0$ and $t_2 = 0.5$), the unstable wave vectors (shaded regions) are preferentially aligned in the k_y direction, giving rise to stripes orthogonal to the y direction.

trated in Fig. 7. In the first case, $Re\,\omega_{\mathbf{k}}$ has two global maxima of the form $\mathbf{k} = (\pm k_x, 0)$. In the second case, $Re\,\omega_{\mathbf{k}}$ has two global maxima of the form $\mathbf{k} = (0, \pm k_y)$. For $\rho_s = \rho_+$, at the bifurcation point, the critical wave vectors are $\mathbf{k}_c = (\pm k_{x_c}, 0)$ when $t_2 = 0$ and $\mathbf{k}_c = (0, \pm k_{y_c})$ when $t_1 = 0$. Further in the instability domain, the fastest growing wave vectors are oriented in the k_x and k_y directions; this means that close enough to criticality, the unstable wave vectors form two disconnected domains aligned in the k_x and k_y directions. Therefore, in the early evolution stage described by the linear analysis, depending upon whether the anisotropy affects inhibition or reproduction, i.e., w_2 or w_1, the orientation of the stripes is orthogonal or parallel to the direction of anisotropy. In order to verify that this behaviour persists when non-linear terms become important in the course of the system evolution, numerical simulations have been performed. Proceeding as explained in Appendix B for the isotropic case, the integro-differential equation (29) is approximated by expanding the densities in Taylor series. The following partial differential equation is obtained:

$$\begin{aligned}\partial_\tau \rho(\mathbf{r},\tau) = &\left[\left(1 + t_1\nabla_y + \tfrac{1}{2}L^2\nabla^2 + \tfrac{1}{2}t_1^2\nabla_y^2\right)\left(\rho(\mathbf{r},\tau)(1 + \Lambda\rho(\mathbf{r},\tau))\right)\right] \\ &\cdot\left[1 - \left(1 + t_2\nabla_y + \tfrac{1}{2}\nabla^2 + \tfrac{1}{2}t_2^2\nabla_y^2\right)\rho(\mathbf{r},\tau)\right] \\ &- \left[\left(1 + t_1\nabla_y\right)\left(\rho(\mathbf{r},\tau)(1 + \Lambda\rho(\mathbf{r},\tau))\right)\right]\cdot\tfrac{1}{6}t_2\nabla_y\left(3\nabla^2 + t_2^2\nabla_y^2\right)\rho(\mathbf{r},\tau) \\ &- \rho(\mathbf{r},\tau)(1 + \Lambda\rho(\mathbf{r},\tau))\cdot\tfrac{1}{24}\left(3\nabla^4 + 6t_2^2\nabla_y^2\nabla^2 + t_2^4\nabla_y^4\right)\rho(\mathbf{r},\tau) \\ &- \mu\rho(\mathbf{r},\tau). \qquad (32)\end{aligned}$$

Typical examples of the patterns obtained by simulating equation (32) with the same domain shape and boundary conditions as in the isotropic case, are given in Figs. 8 and 9. Simulations a_1 and c_1 of Fig. 8 show stripes strictly parallel to the y direction of anisotropy; they model a situation where the anisotropy is only acting on reproduction, i.e., w_1. Simulations a_2 and c_2 of Fig. 8 show what happens when the anisotropy influences inhibition, i.e., w_2, and has no effect on reproduction: one obtains undulating stripes which are oriented at right angle w.r.t. the y direction and which furthermore move upward (in the positive y direction). In Fig. 9, the simulation shows the formation of arcs the main axis of which is orthogonal to the y direction. These arcs move upward; they are obtained when the anisotropy affects inhibition, i.e., w_2.

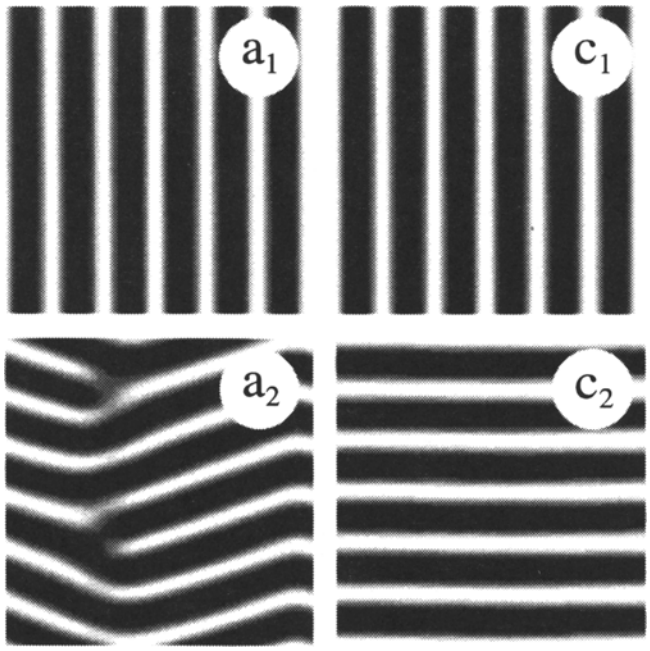

Figure 8. Vegetation patterns in the anisotropic case. We have simulated the influence of anisotropy (in the y direction) on reproduction (patterns a_1, c_1 obtained for $t_1 = 1$ and $t_2 = 0$), and on inhibition (patterns a_2, c_2 obtained for $t_1 = 0$ and $t_2 = 1$). The simulations a_i ($i = 1,2$) correspond ($\mu = 0.95$, $L = 0.1$, $\Lambda = 1$), in the isotropic case, to a banded pattern (cf. Fig. 6a). The simulations c_i correspond ($\mu = 0.95$, $L = 0.1$, $\Lambda = 0.8$), in the isotropic case, to a pattern of hexagonal symmetry (cf. Fig. 6c). Reproduction anisotropy selects stripes parallel to the anisotropy direction and inhibition anisotropy selects stripes orthogonal to that direction, independently of the spatial symmetry properties of the patterns obtained in the isotropic case for the same values of parameters. Parallel stripes are static, while orthogonal stripes are moving upward, i.e., in the positive y direction.

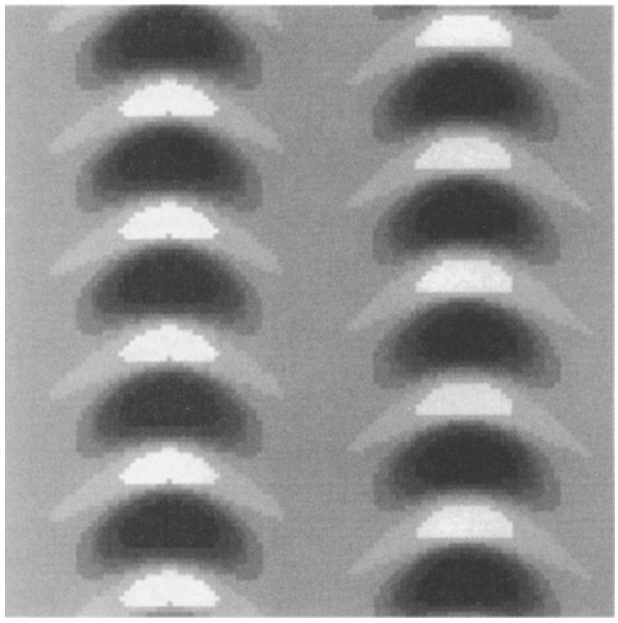

Figure 9. In the case of anisotropic inhibition (in the y direction), arcuate patterns may appear ($\mu = 0.995$, $L = 0.45$, $\Lambda = 1$, $t_1 = 0$ and $t_2 = 2$). They consist of arcs the main axis of which is orthogonal to the anisotropy direction and which move upward (positive y direction).

These results explain several experimental facts not well understood until now. First, they show that roll-like vegetation patterns of both orientations, orthogonal and parallel to the ground slope (considered here as the main direction of anisotropy), as well as vegetation arcs orthogonal to that direction, may originate from the same population dynamics; they are different aspects of the same phenomenon. Second, they show that vegetation patterns (wavy bands and arcs) oriented at right angle w.r.t. the slope of the terrain are moving in the direction of this anisotropy, while vegetation patterns (straight stripes) parallel to that direction are, on the whole, static.

5. Conclusion. The results obtained within the framework of this mean-field description of the evolution of plant communities support the idea that the mechanism of TB formation involves a symmetry breaking instability which leads to the establishment of a spatially periodic distribution of vegetation. This instability is an intrinsic property of the propagation-by-reproduction transport process which governs the spatio-temporal dynamics of plant communities. It appears as a consequence of the fact that the

inter-plant interactions which constitute the basic ingredients of this dynamics are necessarily non-local phenomena: they operate over well-defined ranges, given by the parameters L_i associated to the weighting functions ω_i; it is the value of these interaction ranges which determines the characteristic length of the inhomogeneities which appear. For the instability to be possible, the range of inter-plant interactions described by the inhibition function F_2 must be greater than the cooperative inter-plant interactions described by the reproduction function F_1.

In agreement with field observations, the wavelength predicted by the model for the patterns is a decreasing function of the vegetation density (Gavaud, 1966; White, 1970). This wavelength must be greater than the plant size and, therefore, the patterns are expected in poorly vegetated areas like arid regions where environmental stress is high. Under isotropic conditions, depending on the values of the parameters, the model predicts the emergence of either hexagonal or banded spatial structures and thus that TB may appear even on homogeneous, completely flat territories. Though some authors assert that they have observed stripes of vegetation on flat territories (Clos-Arceduc, 1956; White, 1969), more recent field investigations generally aim at showing that levelled grounds support spotted rather than banded vegetation patterns (Couteron, 1996). The prediction of the model, that TB can develop on virtually flat soils, is therefore not clearly corroborated (or refuted) by existing data. On the other hand, one could speculate that in some cases spotted vegetation patterns correspond to a hexagonal (or parallelogram?) pattern the spot distribution of which is perturbed by random soil irregularities. It would be interesting to investigate this possibility by Fourier analysing aerial photographs.

Remarkably, the model predicts that the same dynamical mechanism can give rise to the two kinds of linear vegetation patterns, parallel and orthogonal to the ground slope (main source of anisotropy), which have been observed *in situ* (Macfadyen, 1950b; White, 1969), and which are traditionally considered to be distinct phenomena (Greenwood, 1957; Boaler and Hodge, 1962; Hemming, 1965). Stripes of vegetation parallel to the ground gradient have been seldom recorded, only in Jordan and Somaliland to our knowledge. The interest taken in these vegetal structures rapidly decreased after their discovery, probably because a clear explanation of their origin, even unformalised, was missing. The model interprets the two types of stripe as distinct aspects of the same vegetation dynamics. Indeed, we have seen here that the presence of an anisotropy can, depending on which kind of inter-plant interactions it affects, either select a pattern constituted of straight stripes parallel to the direction of anisotropy or, on the contrary, select a pattern constituted of undulating bands and arcs orthogonal to that direction. More precisely, if the anisotropy affects reproduction, vegetation patterns of the first type are favoured, while if the

anisotropy affects the inhibition processes, patterns of the second type are favoured. The model predicts also, in contrast with a widespread opinion (Greenwood, 1957), that ground curvature is not a necessary factor to produce vegetation arcs, since they can be obtained for constant ground gradient. Furthermore, it explains why, while vegetation structures parallel to the direction of anisotropy are globally static, patterns orthogonal to that direction may be moving. On a sloping ground, inter-plant inhibition is more important in the upslope direction because plants located downslope can consume some amount of water flowing downward which would be beyond their reach otherwise. This situation has been modeled by translating the inhibition weighting function in the positive y direction representing the upslope direction (the negative y direction corresponding to the downslope direction). We thus find that the patterns obtained in the simulations, which migrate in the positive y direction, correspond in reality to upslope migrating patterns. This behaviour is in agreement with experimental observations (Worrall, 1959; Hemming, 1965; Cornet *et al.*, 1988; Tongway and Ludwig, 1990; Montaña, 1992).

The authors are deeply grateful to Prof. M. Lepage (Ecole Normale Supérieure, Paris) for his interest in this work and for very stimulating discussions.

APPENDIX A

The dispersion relation (17) has a unique zero

$$k_0 = \sqrt{\frac{2 \ln \mu}{L'^2 - L^2}}, \tag{A1}$$

when the parameters μ, L, L' satisfy the condition

$$\frac{\ln \mu}{L'^2 - L^2} > 0, \quad \text{or equivalently} \quad (1 - \mu)(L - L') > 0. \tag{A2}$$

Since the function (17) is continuous in k, the requirement that

$$\lim_{k \to \infty} \omega_k < 0, \tag{A3}$$

reduces in this case to the condition

$$\frac{d\omega_k}{dk}(k_0) = \sqrt{\frac{2 \ln \mu}{L'^2 - L^2}} (L'^2 - L^2) \mu^{L^2/(L^2 - L'^2)} < 0, \tag{A4}$$

which amounts to asking that $L > L'$. On the other hand, when the parameters μ, L, L' fulfill the condition

$$(1-\mu)(L-L') < 0, \tag{A5}$$

the dispersion relation considered has no zero and, by continuity, keeps its sign for all values of k. Condition (A3) is thus also equivalent to

$$\omega_k(0) = 1-\mu < 0, \tag{A6}$$

which, taking inequality (A5) into account, implies $L > L'$.

APPENDIX B

Referring to isotropic environments, this partial-differential-equation version of the model must necessarily be invariant under symmetry operations of rotation. In particular, the symmetry $\mathbf{r} \leftrightarrow -\mathbf{r}$ must be conserved, so that terms corresponding to odd derivatives must cancel out after integration. On the other hand, the dispersion relation describing the linear stability properties of this approximate model has the same properties of invariance in the conjugate space $\mathbf{k}$. Because of the equivalence $\nabla^n \leftrightarrow (i\mathbf{k})^n$ through the Fourier transform, this new dispersion relation is a polynomial in k^2. It is nothing else than the Taylor expansion in k at 0 of the dispersion relation (19). Clearly, this approximate dispersion relation must be a polynomial of at least fourth order in k to recover the instability predicted by equation (12). In other words, it must be of the form $\alpha + \beta k^2 + \gamma k^4$; remembering that the instability corresponds to the existence of a finite band of unstable modes, we must have $\gamma < 0$, $\alpha < 0$ and $\beta > 0$. The agreement between the exact and approximate behaviour can be checked by comparing the dispersion relations for the integral equation with that of its Taylor expansion. We first consider the linear stability of the trivial steady state ρ_0. For the integral equation, it is given by relation (17), where we have set $L' = 0$:

$$\omega_k = \mathrm{e}^{-(L^2k^2/2)} - \mu. \tag{B1}$$

Its Taylor expansion is

$$\omega_k = 1 - \mu - \tfrac{1}{2}L^2k^2 + \tfrac{1}{8}L^4k^4 + O(k^6). \tag{B2}$$

From relation (B1), we see that the modes corresponding to large wave numbers k (or, equivalently, to small wavelengths) are stable: $\omega_k \to -\mu < 0$ for $k \to +\infty$. But in the fourth-order Taylor approximation (B2), there is instability for the same condition, i.e. $\omega_k \to +\infty$ when $k \to +\infty$. We also note that this instability is avoided if the expansion is cut at the second order. Next, we consider the linear stability of the non-trivial stationary states $\rho_s = \rho_\pm$. For the integral equation, it is given by relation (19), whose Taylor expansion is

$$\begin{aligned}\omega_k = {} & (1-\rho_s)(1+2\Lambda\rho_s)(1-\tfrac{1}{2}L^2k^2+\tfrac{1}{8}L^4k^4+O(k^6)) \\ & -\rho_s(1+\Lambda\rho_s)(1-\tfrac{1}{2}k^2+\tfrac{1}{8}k^4+O(k^6)) - (1-\rho_s)(1+\Lambda\rho_s).\end{aligned} \tag{B3}$$

In relation (19), short wavelengths (large wave numbers) are always stable since $\omega_k \to -(1-\rho_s)(1+\Lambda\rho_s) < 0$, for $k \to \infty$. But in relation (B3), if both developments are stopped at the fourth order, this stability holds only for certain values of the parameters, those for which the coefficient of k^4 is negative. This restriction is dodged if the first development is cut at second order. Since the first terms of relations (B1) and (19) come from the first integral in equation (12), we shall thus retain only the second-order terms of the Taylor expansions of the integral representing plant dissemination. In brief, the approximation goes as follows: the development is stopped at second order in the first integral, to have a correct behaviour of the steady state stability, and at fourth order in the second integral representing inhibition effects, to stabilise the large values of k. In making the product of the two integrals, terms are retained up to the fourth order. Within this framework of approximations, we finally obtain equation (28).

REFERENCES

Ambouta, K. 1984. Contribution à l'édaphologie de la brousse tigrée de l'Ouest Nigérien. Thèse de Docteur-Ingénieur, Université de Nancy I.

Audry, P. and Ch. Rossetti. 1996. Is the banded pattern merely a structural expression of an instable pioneer vegetation. Communication at *SALT Int. Symp.*: Banded vegetation patterning in arid and semi-arid environment. Ecological processes and consequences for management. Paris, France. *Acta Oecologica*, to appear.

Beard, J. S. 1967. A study of patterns in some West Australian Heath and Mallee communities. *Aust. J. Bot.* **15**, 131–139.

Bernd, J. 1978. The problem of vegetation stripes in semi-arid Africa. *Plant. Res. and Develop.* **8**, 37–50.

Boaler, S. B. and C. A. H. Hodge. 1962. Vegetation stripes in Somaliland. *J. Ecol.* **50**, 465–474.

Boaler, S. B. and C. A. H. Hodge. 1964. Observations on vegetation arcs in the northern region, Somali Republic. *J. Ecol.* **52**, 511–544.

Clayton, W. D. 1966. Vegetation ripples near Gummi, Nigeria. *J. Ecol.* **54**, 415–417.

Clos-Arceduc, M. 1956. Etude sur photographies aériennes d'une formation végétale sahélienne: la brousse tigrée. *Bull. Inst. Afr. noire Sér. A* **18**, 677–684.

Clos-Arceduc, M. 1964. La géométrie des associations végétales en zone aride. *Act. Conf. UNESCO:* Explorations aériennes et études intégrées. Toulouse, pp. 419–421.

Cornet, A. F., J. P. Delhoume and C. Montaña. 1988. Dynamics of striped vegetation patterns and water balance in the chihuahuan desert. In *Diversity and Pattern in Plant Communities*, H. J. During, M. J. A. Werger and J. H. Willems (Eds), pp. 221–231. The Hague: SPB Academic Publishing.

Couteron, P. 1996. Comparison of spatial patterns of woody species in a spotted savanna and a tiger bush of Northern Yatenga (Burkina Faso, West Africa). Communication at *SALT Int. Symp.*: Banded vegetation patterning in arid and semi-arid environment. Ecological processes and consequences for management. Paris, France.

Cross, M. C. and P. C. Hohenberg. 1993. Pattern formation outside of equilibrium. *Rev. Mod. Phys.* **65**, 851–1112.

Dunkerley, D. and K. Brown. 1996. Banded vegetation near Broken Hill, Australia: significance of surface roughness and soil physical properties. Communication at *SALT Int. Symp.*: Banded vegetation patterning in arid and semi-arid environment. Ecological processes and consequences for management. Paris, France. *Catena*, to appear.

Ehrman, M., S. Galle, J. Seghieri and C. Valentin. 1996. Patterning and pioneer processes of the herbaceous front in a tiger bush. Communication at *SALT Int. Symp.*: Banded vegetation patterning in arid and semi-arid environment. Ecological processes and consequences for management, Paris, France.

Fife, P. C. 1979. *Mathematical Aspects of Reacting and Diffusing Systems. Lecture Notes in Biomathematics*, Vol. 28. Berlin/New York: Springer-Verlag.
Galle, S. and J. Seghieri. 1994. Dynamics of soil water content in relation to annual vegetation: the tiger bush in the sahelian Niger. *Ann. Geophys. Suppl. II* **12**, C443.
Gavaud, M. 1966. Etude pédologique du Niger Occidental. Editions de l'ORSTOM de Dakkar-Hann.
Glover, P. E., E. C. Trump and L. E. D. Wateridge. 1964. Termitaria and vegetation patterns on the Loita plains of Kenya. *J. Ecol.* **52**, 367–377.
Greenwood, J. E. G. W. 1957. The development of vegetation in Somaliland Protectorate. *Geogr. J.* **123**, 465–473.
Greig-Smith, P. 1979. Pattern in vegetation. *J. Ecol.* **67**, 755–779.
Grove, A. T. 1957. Patterned ground in Northern Nigeria. *Geogr. J.* **123**, 271–274.
Gunton, J. D., M. San Miguel and P. S. Sahni. 1983. The dynamics of first order transitions. In *Phase Transitions and Critical Phenomena*, C. Domb and J. L. Lebowitz (Eds), Vol. 8. New York: Academic Press.
Hemming, C. F. 1965. Vegetation arcs in Somaliland. *J. Ecol.* **53**, 57–67.
Humphreys, G. S., J. Eddy, D. M. Hart, P. B. Mitchell and P. C. Fanning. 1996. Vegetation arcs and litter dams: similarities and differences. Poster at *SALT Int. Symp.*: Banded vegetation patterning in arid and semi-arid environment. Ecological processes and consequences for management. Paris, France. *Catena*, to appear.
Ives, R. L. 1946. Desert ripples. *Am. J. Sci.* **244**, 492–501.
Langer, J. S. 1992. An introduction to the kinetics of first-order phase transitions. In *Solids Far from Equilibrium*, C. Godrèche (Ed), pp. 297–363. Cambridge, UK: Cambridge University Press.
Levin, S. A. and L. A. Segel. 1985. Pattern generation in space and aspect. *SIAM Rev.* **27**, 45–67.
Litchfield, W. H. and J. A. Mabbutt. 1962. Hardpan in soils of semi-arid Western Australia. *J. Soil Sci.* **13**, 148–159.
Mabbutt, J. A. and P. C. Fanning. 1987. Vegetation banding in arid Western Australia. *J. Arid Env.* **12**, 41–59.
Macfadyen, W. A. 1950a. Soil and vegetation in British Somaliland. *Nature* **165**, 121.
Macfadyen, W. A. 1950b. Vegetation patterns in the semi-desert plains of British Somaliland. *Geogr. J.* **116**, 199–211.
Mauchamp, A., S. Rambal and J. Lepart. 1994. Simulating the dynamics of a vegetation mosaic: a spatialized functional model. *Ecol. Mod.* **71**, 107–130.
Moloney, K. A. 1986. Wave and nonwave regeneration processes in a subalpine Abies balsamea forest. *Can. J. Bot.* **64**, 341–349.
Montaña, C., J. Lopez-Portillo and A. Mauchamp. 1990. The response of two woody species to the conditions created by a shifting ecotone in an arid ecosystem. *J. Ecol.* **78**, 789–798.
Montaña, C. 1992. The colonization of bare areas in two-phase mosaics of an arid ecosystem. *J. Ecol.* **80**, 315–327.
Murray, J. D. 1993. *Mathematical Biology. Biomathematics Texts*, 2nd ed., Vol. 19. Berlin/New York: Springer-Verlag.
Ouedraogo, P. and M. Lepage. 1996. Termite-soil-vegetation interactions in a striped vegetation pattern, Burkina Faso. Communication at *SALT Int. Symp.*: Banded vegetation patterning in arid and semi-arid environment. Ecological processes and consequences for management. Paris, France. *Acta Oecologica*, to appear.
Ruxton, B. P. and L. Berry. 1960. The Butana grass patterns. *J. Soil Sci.* **11**, 61–62.
Schlesinger, W. H., J. F. Reynolds, G. L. Cunningham, L. F. Huenneke, W. M. Jarrell, R. A. Virginia and W. G. Whitford. 1990. Biological feedbacks in global desertification. *Science* **247**, 1043–1048.
Thiéry, J. M., J.-M. d'Herbès and C. Valentin. 1995. A model simulating the genesis of banded vegetation patterns in Niger. *J. Ecol.* **83**, 497–507.
Tongway, D. J. and J. A. Ludwig. 1990. Vegetation and soil patterning in semi-arid mulga lands of Eastern Australia. *Aust. J. Ecol.* **15**, 23–34.
Turing, A. M. 1952. The chemical basis of morphogenesis. *Phil. Trans. Roy. Soc. Lond., Ser. B* **237**, 37–72.

Valentin, C. and J.-M. d'Herbès. 1996. The Nigerian tiger bush as natural water harvesting system. Communication at *SALT Int. Symp.*: Banded vegetation patterning in arid and semi-arid environment. Ecological processes and consequences for management. Paris, France. *Catena*, to appear.
Van Der Meulen, F. and J. W. Morris. 1979. Striped vegetation patterns in a Transvaal savanna. *Geo-Eco-Trop.* **3**, 253–266.
Vesey-Fitzgerald, D. F. 1957. The vegetation of the Red Sea coast north of Jedda, Saudi Arabia. *J. Ecol.* **45**, 547–562.
White, L. P. 1969. Vegetation arcs in Jordan. *J. Ecol.* **57**, 461–464.
White, L. P. 1970. *Brousses Tigrées* patterns in Southern Niger. *J. Ecol.* **58**, 549–553.
White, L. P. 1971. Vegetation stripes on sheet wash surfaces. *J. Ecol.* **59**, 615–622.
Wickens, G. E. and F. W. Collier. 1971. Some vegetation patterns in the Republic of the Sudan. *Geoderma* **6**, 43–59.
Wilson, J. B. and A. D. Q. Agnew. 1992. Positive feedback switches in plant communities. *Adv. Ecol. Res.* **23**, 263–336.
Worrall, G. A. 1959. The Butana grass patterns. *J. Soil Sci.* **10**, 34–53.
Worrall, G. A. 1960a. Patchiness in vegetation in the Northern Sudan. *J. Ecol.* **48**, 107–115.
Worrall, G. A. 1960b. Tree patterns in the Sudan. *J. Soil Sci.* **11**, 63–67.

Received 23 April 1996
Revised version accepted 8 August 1996